

Accounting for detection probability when estimating force-of-infection from animal encounter data

Paul B. Conn · Evan G. Cooch · Peter Caley

Received: 4 September 2009 / Revised: 19 July 2010 / Accepted: 27 September 2010 / Published online: 3 November 2010
© Dt. Ornithologen-Gesellschaft e.V. (outside the USA) 2010

Abstract Force-of-infection (FOI; the instantaneous rate at which susceptible individuals acquire infection) is an important summary parameter in many disease studies. This parameter controls the propensity of diseases and parasites to spread through populations and often depends on the degree of contact between susceptible and infected individuals. Longitudinal studies are perhaps capable of providing the most information about FOI; however, inference can also be drawn from cross-sectional age-prevalence data in certain situations (for instance, when disease is endemic in a population with little temporal variation in vital rates). In this paper, we provide a review of FOI as it relates to the study of marked animals,

highlighting difficulties with obtaining parameter estimates with the intended interpretation. We also provide several alternatives for accounting for detection probability when estimating FOI. We primarily concentrate on the analysis of cross-sectional age-prevalence data, where previous approaches have traditionally assumed that the probability of sampling an individual is the same regardless of disease status or age class. Since this assumption is likely to be violated in many wildlife populations, we work to extend existing statistical methodology to account for potential differences in capture probability. Our approach requires that data be gathered such that capture–recapture or removal estimators of abundance may be employed. We use simulation to investigate the importance of accounting for differences in detectability, demonstrating a potential for substantial bias when detectability is ignored. Finally, we illustrate our approach by analyzing age-prevalence data from a removal study of ferrets in New Zealand. Interest in this case focused on quantifying age-specific susceptibility of ferrets to bovine tuberculosis.

Communicated by M. Schaub.

Electronic supplementary material The online version of this article (doi:10.1007/s10336-010-0591-z) contains supplementary material, which is available to authorized users.

P. B. Conn (✉)
Laboratory of Ornithology, Cornell University,
159 Sapsucker Woods Road, Ithaca, NY, USA
e-mail: paul.conn@noaa.gov

P. B. Conn
National Marine Fisheries Service,
Southeast Fisheries Science Center,
101 Pivers Island Road, Beaufort, NC, USA

E. G. Cooch
Department of Natural Resources, Fernow Hall,
Cornell University, Ithaca, NY, USA

P. Caley
Risk Sciences Branch, Bureau of Rural Sciences,
Department of Agriculture, Fisheries and Forestry,
M.6.202, 18 Marcus Clarke St, GPO Box 858,
Canberra City, ACT, Australia

Keywords Apparent prevalence · Capture–recapture · Detection probability · Force-of-infection

Introduction

Force-of-infection (FOI) is a critical parameter in many epidemiological models, representing the instantaneous rate at which susceptible individuals become infected (Muench 1959; Cohen 1973; Keiding 1991; Heisey et al. 2006). Its functional form differs depending on the assumptions of the underlying disease model. For instance, when exposure is controlled by environmental factors, FOI may vary by time, age, and duration of exposure, but it

rarely is written as a function of the number of infected individuals in the population. In contrast, when infection is contagious, FOI is often assumed to be dependent on the rate of contact between susceptible and infected individuals, and sometimes in a highly nonlinear manner (for a thorough review see Caley et al. 2009). In this paper, we focus primarily on environmental transmission, which does not require that one know or estimate the number of infected individuals in the population.

The term FOI has been used in two different senses in the disease ecology literature, which may lead to some confusion. Several recent studies (e.g., Lachish et al. 2007; Ozigul et al. 2009) referred to finite state transition probabilities from susceptible to infected states as FOI. Estimated from traditional multistate mark–recapture models (MSMR models; Brownie et al. 1993; Hestbeck et al. 1991; Schwarz et al. 1993), these parameters represent the probability that an individual will be infected at time $t + 1$ given that it was susceptible at time t and survived from $t \rightarrow t + 1$. In MSMR models, survival from $t \rightarrow t + 1$ is usually associated with the state of the animal at a discrete point in time, t . In contrast, conceptualization of FOI as a rate emphasizes that dynamics occur in continuous time, with risks of mortality and infection changing with the state of the individual. In the likely case that mortality and transmission dynamics do both occur continuously, estimators of survival and transition probability from MSMR models will often be biased (Joe and Pollock 2002); with regard to typical epidemiological studies, Joe and Pollock's (2002) results suggest that both FOI and the effect size for disease on survival will be negatively biased. As such, we prefer to define FOI as a rate, rather than a probability, and to build models for disease systems where dynamics occur in continuous time.

Although longitudinal studies using long-term capture–recapture studies may be preferable from an estimation standpoint, ecologists and epidemiologists frequently use apparent prevalence (the percentage of infected individuals in a sample) to gauge the level of disease or parasitic infection in animal and plant populations. However, raw apparent prevalence is sensitive to the age-structure of the population and to the censoring effects of infection-mediated mortality (Heisey et al. 2006). For example, younger individuals have less time to become infected, so prevalence of infection is typically lower in younger organisms than with older ones. Further, if infected individuals die considerably sooner than uninfected ones, raw prevalence may give an inaccurate picture of the importance of a pathogen because living organisms are less likely to be infected. To combat these problems, FOI models have become a common way to analyze prevalence data when age can be determined at the time of the sample and when disease is endemic in a population. These models are often parameterized in terms of hazard rates and permit estimation of age-specific

transmission and mortality rates that account for the biasing effects of age and infection-induced mortality. Frequently used in human epidemiology (see review by Heisey et al. 2006), this type of analysis has also been employed in fish and wildlife disease studies (e.g., Cohen 1973; Woolhouse and Chandiwana 1992; Hudson and Dobson 1997; Caley and Hone 2002; Heisey et al. 2006; Gauthier et al. 2008).

In sampling animal and plant populations, it is often difficult to obtain a complete census of the population. In these cases, age-prevalence data are almost always summarized from a sample of the population and treated as if they represent the population as a whole. However, when the probability of detecting an organism depends on age- or stage-class (as with disease status), age-prevalence in the sample may differ markedly from age-prevalence in the population (Jennelle et al. 2007). For instance, infection may induce behavioral changes that make them more or less prone to being captured (Faustino et al. 2004; Jennelle et al. 2007). Even in plants, a seemingly ideal organism for this type of study, detectability can be less than one and may differ by life-state (Kery and Gregg 2003).

Jennelle et al. (2007) have described how to correct prevalence for differences in detection probability if estimates of detection probabilities are available. However, treating corrected prevalence as data for fitting FOI models is akin to doing statistics on statistics. A better approach is to embed the process model for disease dynamics directly into a model for the sampling process. In this manner, estimates of FOI parameters and accompanying measures of precision would implicitly account for uncertainty associated with detection probability and thus for uncertainty about true age-prevalence at the population level.

In this paper, we outline several approaches for estimating FOI with data from marked animals. We start by making suggestions on how traditional MSMR models can be reparameterized to allow inference about instantaneous FOI. Our focus then turns to ways of analyzing cross-sectional age-prevalence data when detectability has the potential to differ by age or infection status. In this case, we assume that the investigator has collected age-prevalence data in a manner that facilitates the estimation of detection probability. In particular, we concentrate on the case where mark–recapture or removal sampling is employed, with the goal of estimating infection-mediated mortality and transmission rates. After developing a statistical framework, we employ a simulation study to investigate estimator properties under several biological and sampling scenarios, comparing our approach to a more traditional approach that does not attempt to account for detectability. Finally, we analyze data from a removal study of feral ferrets *Mustelo furo* in New Zealand, where interest is in estimating epidemiological parameters associated with bovine tuberculosis *Mycobacterium bovis* infection.

Statistical framework

Multistate mark–recapture models revisited

Canonical MSMR models have traditionally assumed that state transitions occur at the end of survival intervals, so that susceptible individuals at time t have the same survival probability to $t + 1$ regardless of whether they become infected or not. Joe and Pollock (2002) showed that when state transitions are possible between t and $t + 1$, and when survival probability is different for the two states, (1) the state transition probability estimator (i.e., estimate of infection probability in our case) is negatively biased, and (2) estimates of mortality are biased (the state with lower survival probability exhibiting positive bias, and the state with the higher survival probability exhibiting negative bias). Relative bias was mostly low (<10%) for the cases they considered; however, transition probabilities were assumed to be symmetric (i.e., the transition from state A to state B was the same as for state B to state A). Further, only one such transition was allowed between successive sampling periods. The potential for bias when applied to disease studies is possibly much higher, as state transitions are often unidirectional.

To be more consistent with the usual interpretation of FOI, we suggest reparameterizing MSMR models in terms of instantaneous rates [i.e., hazards; Cox and Oakes (1984)]. A general strategy to accomplish this is to assume that state transitions (including death) occur according to a finite state continuous time (FSCT) Markov process (Taylor and Karlin 1984); note that FSCT processes are also termed “multistate” processes in the medical literature. Recently invoked by Miller and Andersen (2008) to model fish tagging experiments in continuous time, FSCT modeling involves constructing a matrix of homogeneous, infinitesimal hazard rates (if hazards vary as a function of time, piecewise constant hazard models may be assumed). For example, letting δ denote the instantaneous mortality rate for susceptible individuals, $\delta + \mu$ be the instantaneous mortality rate for infected individuals, and λ be the infection hazard (i.e., force-of-infection) and imposing a three-state irreversible disease model (e.g., Keiding 1991; Heisey et al. 2006; see Fig. 1), the corresponding infinitesimal matrix is given by

$$\mathbf{A} = \begin{bmatrix} -(\lambda + \delta) & \lambda & \delta \\ 0 & -(\delta + \mu) & \delta + \mu \\ 0 & 0 & 0 \end{bmatrix}.$$

Each row corresponds to the state of an individual at the beginning of the time period, with off-diagonal entries set to the hazard rate for moving to the state given by its column number. Diagonal entries are then set so that each row sums to zero. A matrix of Arnason–Schwarz state

A 3 state irreversible disease model

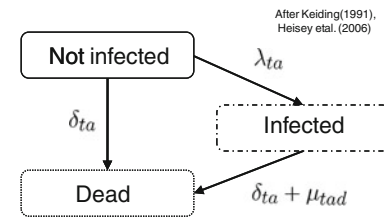


Fig. 1 Depiction of a three-state irreversible disease system, where instantaneous transition hazards are denoted by λ (force-of-infection), δ (mortality rate for susceptible individuals) and $\delta + \mu$ (mortality rate for infected individuals). Subscripts t and a denote time and age, respectively. After Keiding (1991) and Heisey et al. (2006)

transition parameters ϕ (Arnason 1972, 1973; Schwarz et al. 1993) may then be written in terms of hazard rates by calculating $\mathbf{P} = \mathbf{V} \exp(\mathbf{D}t_{\Delta})\mathbf{V}^{-1}$, where t_{Δ} denotes the duration of the time interval, \mathbf{D} denotes a diagonal matrix of the eigenvalues of \mathbf{A} , and \mathbf{V} is the matrix of eigenvectors of \mathbf{A} (Kalbfleisch and Lawless 1985; Miller and Andersen 2008). Covariates thought to influence disease progression (e.g., age, time) could potentially be incorporated through proportional hazard models (Cox and Oakes 1984). The interested reader is referred to Miller and Andersen (2008) for further explanation.

Age-prevalence modeling

Many studies of FOI base inference on cross-sectional age prevalence samples. For instance, a researcher might sample a population at a single point in time and obtain counts of the number of infected and non-infected individuals at a given age. Letting C_a^I and C_a^N denote the number of age a infected and non-infected individuals in a sample, age-specific apparent prevalence is then computed as $\frac{C_a^I}{C_a^I + C_a^N}$. Assuming that the sample is much smaller than the population size (thus ignoring finite population adjustments), one approach for analyzing FOI would be to impose a binomial model for these counts (e.g., Caley et al. 2009), i.e.,

$$C_a^I \sim \text{Binomial}(C_a^I + C_a^N; v_a).$$

Here, $\text{Binomial}(\theta_1; \theta_2)$ represents a binomial probability mass function with index (number of trials) θ_1 and success probability θ_2 , and v_a denotes true prevalence in the population ($v_a = \frac{N_a^I}{N_a^I + N_a^N}$, where N_a^I and N_a^N give age-specific abundance of infected and non-infected individuals, respectively). Inference about FOI is then obtained by placing ultrastructural constraints on the v_a parameters.

The problem is that this approach ignores any bias or additional variability associated with possible differences in detection probability between infected and non-infected individuals. Assuming that the detection probability for

infected and non-infected individuals are p_a^I and p_a^N , the expected count of each group is given by $E(C_a^I) = N_a^I p_a^I$ and $E(C_a^N) = N_a^N p_a^N$. If one does not account for possible differences in detection probability, a first order approximation to $E(\hat{v}_a)$ may then be given by

$$E(\hat{v}_a) \approx \frac{N_a^I p_a^I}{N_a^I p_a^I + N_a^N p_a^N}.$$

If $p_a^I \approx p_a^N$, \hat{v}_a provides a reasonable proxy for v_a ; however, if this condition does not hold, inference based on \hat{v}_a could be misleading.

In practice, there are a priori reasons to expect differences in detection probability. For example, Gauthier et al. (2008) speculated that fish trawls may sample diseased striped bass more often than healthy ones because infection debilitates the host, making them less likely to avoid the sampling gear. Similarly, studies of conjunctivitis in house finches have indicated that infected individuals stay closer to food sources, such as bird feeders (Dhondt et al. 2005), and thus may be more likely to be detected than non-infected individuals. If observations at bird feeders are used to make inferences about disease prevalence or FOI, the results may be misleading. Jennelle et al. (2007) discuss the ramifications of this problem for the interpretation of raw prevalence; our goal in future sections is to explore the consequences of using such data for FOI modeling and to outline a solution.

Ignoring detection probability when estimating FOI

The binomial model for counts in the previous section implies a joint likelihood for observed data of the form $\mathcal{L}_1 = [v|\mathbf{C}^I, \mathbf{C}^N]$, where bold symbols denote vectors of parameters or statistics and where the notation $[X|Y]$ denotes the conditional distribution of X given Y . To make inferences about epidemiological parameters of interest (e.g., FOI), one must write v_a as a function of infection and death processes. For cross-sectional data, this typically involves making a stability assumption to ensure that the parameters are identifiable. For example, in the three-state irreversible disease model (Fig. 1), one might assume that disease is endemic in the population and that temporal variation in vital rates is negligible. We proceed by making these assumptions in the rest of this treatment.

Suppose that system dynamics are described by the system of differential equations

$$dN^N/da = -\lambda_a N^N - \delta N^N \tag{1}$$

$$dN^I/da = \lambda_a N^N - \delta N^I - \mu N^I \tag{2}$$

(also see Fig. 1), where age is used in place of time to emphasize that it is the relative numbers of individuals in each disease class from each cohort (those animals born at

the same time) that are of interest. In this case, several possibilities exist for modeling FOI using count data. If we assume that infection does not influence mortality (i.e., $\mu = 0$), v_a can be written as

$$v_a = 1 - \exp\left(-\int_{t=0}^{t=a} h_\lambda(t|\xi) dt\right),$$

where $h_\lambda(t)$ denotes a function describing how λ changes as a function of age and an unknown parameter vector ξ (Caley et al. 2009). Inference about FOI in this case means conducting statistical inference with regard to $\mathcal{L}_2 = [\xi|\mathbf{C}^I, \mathbf{C}^N]$.

Further complexity may be introduced by allowing mortality rates to differ. Allowing $\mu \geq 0$ in Fig. 1, Heisey et al. (2006) showed that one could conduct inference on both ξ and μ using cross-sectional data. If a parametric hazard function is provided for λ_a (say with parameters ζ), Heisey et al. (2006) showed that this probability could be written generically as

$$v_a = 1 - \frac{S_\lambda(0, a)}{S_\lambda(0, a) + \int_0^a f_\lambda(w) S_\mu(w, a) dw}, \tag{3}$$

where $f_\theta(w)$ gives the failure time density function for the process θ , and $S_\theta(x, y)$ gives the survivor function for the process θ given that the organism is alive at x : $\Pr(T_\theta \geq y | T_\theta > x)$ (see, for example, Cox and Oakes 1984). Heisey et al. (2006) showed how to perform inference for a variety of choices for hazard rates, approximating them with piecewise exponential models to evaluate the integral in Eq. (3). They used this approach to estimate ζ and μ in the two-state irreversible disease problem by conducting inference with regard to the likelihood $\mathcal{L}_3 = [\xi, \mu|\mathbf{C}^I, \mathbf{C}^N]$. Note that the generic FSCT approach outlined in section “Statistical framework” could also have been used here to come up with a numerical approximation to v_a .

Accounting for detection probability when estimating FOI

When sampling probabilities depend on disease status, the preceding approach to FOI may no longer suffice. We propose a change in model structure to accommodate potential differences in detection probability. In particular, if data are collected according to a closed capture mark–recapture sampling protocol, we suggest passing the parameters of interest up a level in the modeling hierarchy. For instance, for the three-state irreversible disease model (Fig. 1), a generic likelihood may be written as

$$\mathcal{L}_4 = [\xi, \mu|\mathbf{N}^I, \mathbf{N}^N][\mathbf{N}^I, \mathbf{N}^N, \mathbf{p}^I, \mathbf{p}^N|Data]. \tag{4}$$

The first component of the likelihood, $[\xi, \mu|\mathbf{N}^I, \mathbf{N}^N]$ may be parameterized in a manner analogous to traditional FOI

models (replacing the count vectors \mathbf{C}^I and \mathbf{C}^N with \mathbf{N}^I and \mathbf{N}^N , respectively). The second component, $[\mathbf{N}^I, \mathbf{N}^N, \mathbf{p}^I, \mathbf{p}^N | \text{Data}]$, may be modeled as a mark–recapture or removal study, depending on what sampling protocol was followed. Note that if data are gathered in this manner, \mathbf{C}^I and \mathbf{C}^N are no longer sufficient statistics; rather, encounter histories are modeled. Inference may then proceed by providing explicit forms for each component of the likelihood. Capture–recapture data are clearly desirable as they permit inferences about temporal variation in detectability (Otis et al. 1978). In this case, a diverse array of closed population likelihoods are available (e.g., Otis et al. 1978; Pledger 2000; Conn et al. 2006). However, in certain situations, political and logistical considerations may preclude releases of diseased individuals back into the population. In our study system, for example, individuals were sacrificed to enable disease determination. Thus, in some cases, removal studies may be the only possibility. The likelihood for removals in this case is similar to the one attributable to Zippin (1956):

$$\begin{aligned}
 [\mathbf{N}^I, \mathbf{N}^N, \mathbf{p}^I, \mathbf{p}^N | \mathbf{u}] &= \prod_{a=1}^A \frac{N_a^I!}{u_{1a}^I! u_{2a}^I! \dots u_{Ta}^I!} [p_a^I]^{u_{1a}^I} [(1-p_a^I)p_a^I]^{u_{2a}^I} \\
 &\times [(1-p_a^I)^2 p_a^I]^{u_{3a}^I} \dots [(1-p_a^I)^{T-1} p_a^I]^{u_{Ta}^I} \\
 &\times \prod_{a=1}^A \frac{N_a^N!}{u_{1a}^N! u_{2a}^N! \dots u_{Ta}^N!} [p_a^N]^{u_{1a}^N} [(1-p_a^N)p_a^N]^{u_{2a}^N} \\
 &\times [(1-p_a^N)^2 p_a^N]^{u_{3a}^N} \dots [(1-p_a^N)^{T-1} p_a^N]^{u_{Ta}^N}.
 \end{aligned}
 \tag{5}$$

Here, u_{ta}^I and u_{ta}^N give the number of age a organisms encountered and removed from the population at sampling occasion t that are infected and not infected, respectively, and T gives the total number of sampling occasions. As with all closed encounter models, the use of such a model requires that sampling occasions are close enough together temporally as to preclude any change in the population with regard to infection status, mortality, immigration, emigration, and recruitment.

Simulation study

We conducted a simulation study to compare the performance of our approach to methods not accounting for detectability. We were particularly interested in percent relative bias (%Bias), coefficient of variation (CV), 95% confidence interval coverage (CIcov), and root mean squared error (RMSE) of estimators of λ and μ for the two different approaches. We anticipated that estimator performance would vary as a function of a number of factors, but for simplicity, we considered estimator performance related to

Table 1 Possible inputs to the force-of-infection (FOI) simulation experiment

Capture probability	N_0	A	$HazMod$
$p^N = 0.3, p^I = 0.3$	500	5	Weibull (0.2, 1) (flat)
$p^N = 0.2, p^I = 0.4$	1,000	10	Weibull (0.2, 1.1) (increasing)
$p^N = 0.4, p^I = 0.2$		15	Weibull (0.2, 0.9) (decreasing)
$p^N = 0.1, p^I = 0.5$			Log-logistic (0.3, 2.0) (unimodal)
$p^N = 0.5, p^I = 0.1$			

A complete factorial design was considered where 100 replicates were run for each possible combination of input values

Simulations could vary by capture probability for infected (p^I) and uninfected (p^N) individuals, expected number of births per year (N_0), number of age classes (A), and parametric form of the hazard model for λ ($HazMod$)

variation in (1) detection probability for infected and non-infected organisms, (2) expected number of annual births, (3) the specified hazard function for transmission rate, and (4) the number of age classes that were modeled. We implemented a complete factorial design (Table 1), with 100 replicates at each combination of simulation input values.

We employed a stochastic simulation approach to generate data from the coupled differential equations specified in Eqs. (1) and (2) (Renshaw 1991). All processes were simulated as if they were piecewise exponential, with 20 windows per age increment to approximate age dependency in disease transmission dynamics (the hazard rate at the midpoint of each window was used and assumed to be constant over the entire window). The number of births in a given year was assumed to follow a Poisson distribution, with expectation dependent upon the simulation input value. All simulations assumed that age did not influence detection probability, natural mortality, or infection-associated mortality (note that the latter two assumptions are necessary for estimation with a single snapshot of cross-sectional age-prevalence data). A constant natural mortality hazard of $\delta = 0.1$ and a constant infection-associated hazard of $\mu = 0.3$ were assumed throughout (these values translate into annual survival probabilities of 0.67 and 0.90 for infected and non-infected individuals, respectively). Each simulation was run for A years, and once \mathbf{N}^N and \mathbf{N}^I had been generated, removal encounter histories were then simulated by applying specified capture probabilities to the multinomial model in Eq. (5). All simulations assumed four trapping sessions in the terminal year. These summaries were used to estimate abundance, capture probability, and disease dynamics parameters from Eq. (4); the total number of individuals captured by disease status and age were used as sufficient statistics to estimate parameters from the “traditional” FOI likelihood, \mathcal{L}_3 .

For each simulation, maximum likelihood estimates were computed using function nlm in program R (R

Development Core Team 2005). For simplicity, the same functional form for λ was used for estimation as was used for generation of the data. Numerical variance estimates were computed by inverting the resultant Hessian and applying the delta method (Seber 1982). For each design point and estimation procedure, we recorded the number of simulation replicates yielding proper variance–covariance matrices (i.e., the Hessian was non-singular, and variance estimates were all ≥ 0). Only simulations resulting in proper variance–covariance matrices were used in computation of estimator performance statistics (e.g., bias, CIcov, CV, RMSE). Approximate 95% confidence intervals (CI) were computed as the maximum likelihood estimate ± 2 standard errors (SE). Estimator performance statistics were tabulated with respect to μ , ρ , and κ , where ρ and κ were the parameters associated with the parametric hazard function for λ_a [See Appendix, Electronic Supplementary Material (ESM)]. The requisite code for performing simulations is included in the ESM.

The simulations confirmed extreme bias (up to 45%) in the estimators of parameters of the hazard function for the

transmission rate, λ_a , when detectability varied by infection status and was not accounted for (See Table 1 of Appendix in ESM). In contrast, bias for the approach accounting for detectability (e.g., Eq. 4) was considerably less and, for most cases, statistically indistinguishable from zero. Substantial (up to 35%) positive bias in μ , the rate of disease-mediated mortality, was evident in both approaches when the number of age classes was low ($A = 5$), but it persisted at lower levels as the number of age classes increased for the approach ignoring detectability.

Because bias in parameters for λ_a is difficult to visualize, we simulated several large datasets to provide the reader with a better picture of the consequences of such bias. For the case where $A = 10$ and $N_0 = 100,000$, we simulated one dataset for each combination of capture probability and hazard function type (see Table 1). The value for N_0 was chosen so as to obtain approximate expected value data, thus limiting the influence of sampling variability. When detectability is accounted for, bias in λ_a hazard profiles is minimal, but it is potentially substantial when differences in detectability are ignored (Fig. 2).

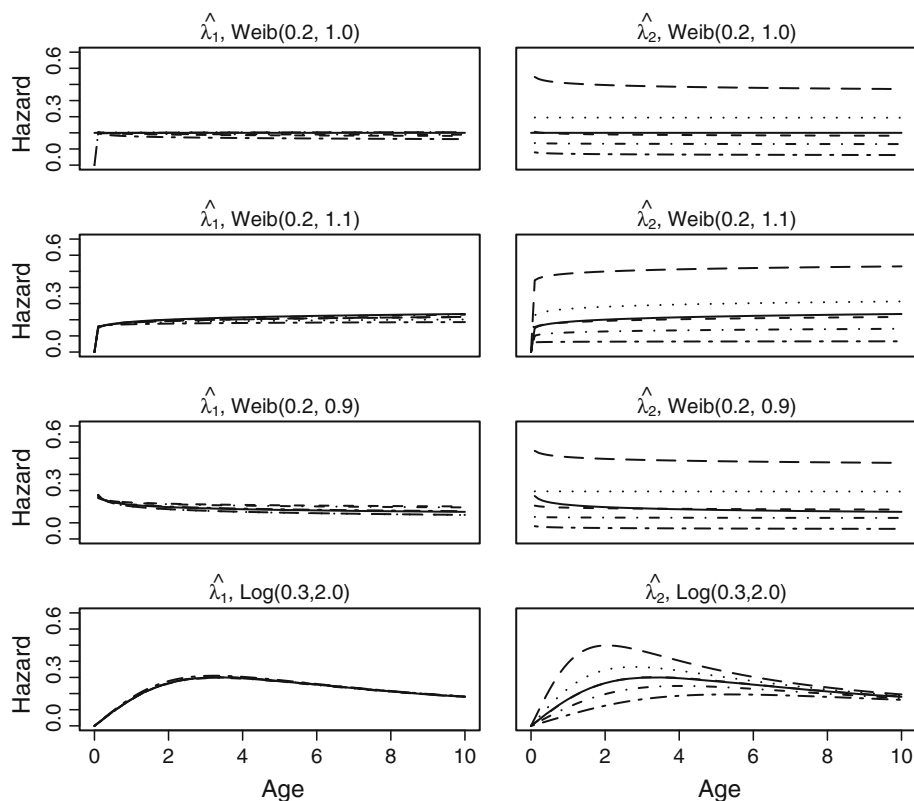


Fig. 2 A visual depiction of hazard profiles resulting from the analysis of large datasets. If λ_1 appears in the graph subtitle, this indicates that the analysis accounting for detection probability was employed, while a λ_2 indicates that detection probability was not accounted for. The true, underlying parametric hazard model is also presented as a *solid black line*. The remaining *lines* on each graph represent estimated hazard profiles under different combinations of

detection probabilities: $p^N = 0.3$ and $p^I = 0.3$ (*broken line, short dashes*), $p^N = 0.2$ and $p^I = 0.4$ (*dotted line*), $p^N = 0.4$ and $p^I = 0.2$ (*broken line, dots/short dashes*), $p^N = 0.1$ and $p^I = 0.5$ (*broken line, long dashes*), and $p^N = 0.5$ and $p^I = 0.1$ (*broken line, dots/long dashes*). p^I Capture probability for infected individuals, p^N capture probability for noninfected individuals. See text for other notations

Table 2 Large sample estimates of the disease-mediated mortality rate when possible variation in detectability was ($\hat{\mu}_1$) and was not ($\hat{\mu}_2$) accounted for

Capture Probability	HazMod	$\hat{\mu}_1$	$\hat{\mu}_2$
$p^N = 0.3, p^I = 0.3$	Weibull(0.2, 1.0)	0.29	0.29
$p^N = 0.3, p^I = 0.3$	Weibull(0.2, 1.1)	0.31	0.31
$p^N = 0.3, p^I = 0.3$	Weibull(0.2, 0.9)	0.29	0.29
$p^N = 0.3, p^I = 0.3$	Log-Logistic(0.3, 2.0)	0.29	0.29
$p^N = 0.2, p^I = 0.4$	Weibull(0.2, 1.0)	0.29	0.38
$p^N = 0.2, p^I = 0.4$	Weibull(0.2, 1.1)	0.35	0.50
$p^N = 0.2, p^I = 0.4$	Weibull(0.2, 0.9)	0.31	0.35
$p^N = 0.2, p^I = 0.4$	Log-Logistic(0.3, 2.0)	0.29	0.27
$p^N = 0.4, p^I = 0.2$	Weibull(0.2, 1.0)	0.30	0.24
$p^N = 0.4, p^I = 0.2$	Weibull(0.2, 1.1)	0.31	0.21
$p^N = 0.4, p^I = 0.2$	Weibull(0.2, 0.9)	0.31	0.27
$p^N = 0.4, p^I = 0.2$	Log-Logistic(0.3, 2.0)	0.30	0.34
$p^N = 0.1, p^I = 0.5$	Weibull(0.2, 1.0)	0.24	0.00
$p^N = 0.1, p^I = 0.5$	Weibull(0.2, 1.1)	0.32	0.06
$p^N = 0.1, p^I = 0.5$	Weibull(0.2, 0.9)	0.28	0.03
$p^N = 0.1, p^I = 0.5$	Log-Logistic(0.3, 2.0)	0.30	0.02
$p^N = 0.5, p^I = 0.1$	Weibull(0.2, 1.0)	0.29	0.17
$p^N = 0.5, p^I = 0.1$	Weibull(0.2, 1.1)	0.31	0.12
$p^N = 0.5, p^I = 0.1$	Weibull(0.2, 0.9)	0.29	0.22
$p^N = 0.5, p^I = 0.1$	Log-Logistic(0.3, 2.0)	0.29	0.42

Each simulation employed initial cohort sizes of $N_0 = 100,000$ to limit the influence of sampling variation, used a true value of μ of 0.3, and 10 age classes. Datasets varied by the assumed capture probability for infected (p^I) and non-infected (p^N) individuals, and the underlying parametric hazard model (*HazMod*)

Large sample bias was also minimal for μ when detectability was accounted for, but this was not the case when detectability was ignored (Table 2).

In addition to bias, we also examined the influence of simulation inputs and analysis methods on small sample CIcov (see Appendix Table 2 ESM), CV (see Appendix Table 3 ESM), and RMSE (see Appendix Table 4 ESM). Values of CIcov were often lower than 95% for both analysis approaches, but they were particularly poor for the scale parameter of hazard rate functions (ρ) when detection rates were highest for infected individuals and when estimation did not account for differences in detectability. In some of these cases, CIcov dropped to zero, such that no estimated CI included the true value of ρ .

The CV was comparable between analysis methods, albeit slightly smaller on average for the approach not incorporating detectability. For μ , CV was unacceptably high with only five age classes (>4.5 in all cases). Interpretation of CV, particularly for μ , was somewhat problematic due to the influence of a number of outliers where estimated variances were quite high. For example, in the first row of Table 3 of the Appendix in the ESM, the entry for CV ($\hat{\mu}_1$) is 34.70; however, 68 out of 85 simulation

replicates had an estimated CV <7.0. As was expected, CV decreased as the number of age classes increased and as the expected number of sampled animals increased. Nevertheless, CV was often >1.0 for μ , and >0.2 for ρ and κ .

The RMSE is perhaps the best indicator of which analysis method to choose because it incorporates both bias and variance. When the probability of detection was equal for infected and noninfected individuals, the RMSE was similar for both analysis methods, indicating that either method of analysis might be chosen. However, as the detection probability for the two states diverged, RMSE increasingly favored the approach accounting for detectability (see Appendix Table 4 ESM).

Feral ferrets and *M. bovis* infection in New Zealand

Caley and Hone (2002) estimated FOI parameters for feral ferrets in New Zealand, comparing support for several transmission alternatives using Akaike’s information criterion (AIC) (Burnham and Anderson 2002). These researchers found support for a model consistent with the hypothesis of dietary-related transmission resulting from the consumption of *M. bovis*-infected material (e.g., from infected brushtail possums *Trichosurus vulpecula*). Their analysis employed \mathcal{L}_3 , assuming that detection probability did not vary with disease state.

We analyzed trapping data from one of Caley and Hone’s (2002) study sites, Awatere Valley, attempting to account for possible differences in detection probability. The study area was sampled in March of 2000 using baited leg-hold traps, and resulting data were summarized by age, disease status, and trapping occasion (Table 3; for further information see Caley and Hone 2002).

Table 3 Number of removals by age (years) and trapping period for feral ferrets not infected and infected with *Mycobacterium bovis*

Age	Trapping occasion								
	1	2	3	4	5	6	7	8	9
Not infected									
0.33	5	3	1	4	1	2	0	1	0
1.33	0	0	0	0	0	0	0	0	0
2.33	1	0	0	0	0	0	0	0	0
3.33	0	0	0	0	0	0	0	0	0
4.33	0	0	0	0	0	0	0	0	0
Infected									
0.33	1	2	3	2	2	2	2	0	2
1.33	1	1	1	0	1	1	0	0	1
2.33	0	0	0	2	0	0	0	0	0
3.33	1	0	1	0	0	0	0	0	0
4.33	0	0	2	0	1	0	0	0	0

We made several modifications to \mathcal{L}_4 for analysis of the ferret data. To start, parameters N_a^N and N_a^I were replaced with $M_a^N + f_a^N$ and $M_a^I + f_a^I$, where M_a^N and M_a^I were the number of animals of each age and disease class, respectively, removed during the study, and f_a^N and f_a^I were nonnegative parameters indicating the difference between true abundance and the total number removed. A log link was used to constrain these parameters to be nonnegative.

We fit a total of 12 models to the ferret data and included two possibilities for detection probability [dependent or not dependent on infection status; denoted as $p(I)$ and $p(\cdot)$, respectively], two possibilities for mortality {ferret mortality affected [$S(I)$] or not affected [$S(\cdot)$]}, and three underlying FOI models. In particular, we considered age-specific FOI models (Weibull, log-logistic, or exponential). The exponential model posits a constant FOI with age, the Weibull model allows monotonically decreasing or increasing FOI hazards with age, and the log-logistic model allows a unimodal distribution for FOI. Given that the youngest individuals sampled at this study area had already been weaned, the exponential model corresponds to the model with the most support from Caley and Hone's (2002) original analysis. Resultant model fits were compared with the conditional AIC (AIC_c) (Burnham and Anderson 2002).

Model fitting suggested that a model with constant infection hazard, constant detection probability, and mortality independent of infection had the most support (Table 4). However, ferret data were quite sparse, which likely led to the selection of models with few parameters. Log-likelihoods were similar for all models fit, and several candidate models had reasonable support. The FOI estimate from the highest ranked model indicated that the FOI hazard was constant at 0.30, with a SE of 0.21 (the SE was estimated by setting abundance parameters (f^I, f^N) that were estimated on the boundary to zero to promote Hessian convergence).

Discussion

We have outlined methods for modeling FOI using animal encounter data that account for potential differences in detection probability by disease status. For longitudinal studies, we suggest that multi-state mark–recapture models are appropriate, but argue that increased realism is imparted by modeling state transitions (including death) using continuous time hazard functions. This is quite similar to the approach used by Ergon et al. (2009) in modeling the latent time of maturation with mark–recapture methods. However, the approach we advocate is more general and does not require that one solve for cell probabilities analytically. Rather, the continuous time FSCT algorithm requires only that one specify an instantaneous transition

Table 4 Models fit to ferret age-prevalence data, ranked by AIC_c

Model	k	$-\text{LogL}$	ΔAIC_c
$\lambda(\text{Exponential})S(\cdot)p(\cdot)$	12	−52.36	0.0
$\lambda(\text{Exponential})S(\cdot)p(I)$	13	−51.54	2.2
$\lambda(\text{LogLogistic})S(\cdot)p(\cdot)$	13	−52.11	3.4
$\lambda(\text{Weibull})S(\cdot)p(\cdot)$	13	−52.28	3.7
$\lambda(\text{Exponential})S(I)p(\cdot)$	13	−52.36	3.9
$\lambda(\text{LogLogistic})S(\cdot)p(I)$	14	−51.36	6.0
$\lambda(\text{Weibull})S(\cdot)p(I)$	14	−51.51	6.3
$\lambda(\text{Exponential})S(I)p(I)$	14	−51.54	6.3
$\lambda(\text{LogLogistic})S(I)p(\cdot)$	14	−52.03	7.3
$\lambda(\text{Weibull})S(I)p(\cdot)$	14	−52.28	7.8
$\lambda(\text{LogLogistic})S(I)p(I)$	15	−51.28	10.1
$\lambda(\text{Weibull})S(I)p(I)$	15	−51.51	10.6

Difference from top ranked conditional Akaike's information criterion (AIC_c) model is given by ΔAIC_c . Also presented are the number of parameters (k) and the negative log-likelihood value ($-\text{LogL}$). Model description includes the functional form for FOI (exponential, Weibull, log-logistic), parameterization for survival, indicating whether there was increased mortality for infected animals [$S(I)$] or not [$S(\cdot)$], and parameterization for detection probability, with $p(\cdot)$ indicating equal detectability among disease states and $p(I)$ indicating that the detection probability depended on disease status

matrix \mathbf{A} for the process (perhaps considering a number of such matrices if hazards vary over time or age). This approach is applicable to a wide variety of disease systems, not just the three-state irreversible disease model.

For cross-sectional age-prevalence data obtained at a snapshot in time, our simulation experiment revealed the importance of accounting for detectability when capture rates differ between infected and non-infected individuals. In particular, the approach accounting for detectability was relatively unbiased with lower mean squared error than the approach ignoring detectability. In practice, researchers will often not know if such a difference exists; in these situations, we recommend that ecologists collect auxiliary data that can be used to estimate detection probabilities.

The simulation study employed here compared estimators of disease dynamics parameters when removal studies were employed. However, the only real requirement is a closed captures model [$\mathbf{N}^I, \mathbf{N}^N, \mathbf{p}^I, \mathbf{p}^N \mid \text{Data}$] that permits inference about abundance and encounter probabilities. In general, removal sampling is less efficient and requires more stringent assumptions about variation in encounter probability than capture–recapture studies. Thus, we would expect better performance of estimators with capture–recapture data and would recommend the use of capture–recapture over removal experiments when it is politically and logistically feasible to release diseased animals back into the population.

Whatever sampling design is chosen, our simulation results indicate that adequate precision on disease dynamics

parameters will typically only be achieved with a large number of age classes and a large number of captured individuals. Out of the range of input parameter values, ten age classes seemed acceptable for disease transmission parameters, while 15 or more may be needed to obtain reasonable precision on disease-mediated mortality, μ . Because ageing individuals is rarely a precise procedure, a reasonable question for future research is whether biased or imprecise ageing techniques have an effect on estimator performance. Although ageing errors can be corrected for if there are some individuals of known age (e.g., Conn and Diefenbach 2007), adding another source of uncertainty to estimation will only decrease estimator precision. A related issue is the degree to which false negatives and positives occur; this problem may be similarly addressed using clinical studies in which a “gold standard” is available to estimate the probabilities of correctly assigning disease status. Although we did not explore the effect of unmodeled age-related differences in detection probability on the FOI estimator, this source of variation could also be addressed using our modeling approach. We suspect that age-based variation in detection rates will only bias traditional FOI estimation if age interacts with disease status in some fashion, since age-specific apparent prevalence is unaffected if both disease classes are impacted similarly by age-related variation in detection probability.

The results in this study were obtained using direct maximization of Eq. 4, which yielded unbiased estimates but slight overestimates of precision (as suggested by the less than nominal CI_{cov}). In the future, a more cohesive approach would be to integrate out unobserved abundance parameters using a method such as MCMC. This approach should do a better job of properly accounting for uncertainty.

Our analysis of feral ferret data suggested a value of FOI ($\hat{\lambda} = 0.30$, SE 0.21) that was commensurate with the values estimated in Caley and Hone’s (2002) original study. Model selection favored a model with a constant detection probability and also suggested that the FOI hazard was constant over time for the observed age classes (the latter result is consistent with Caley and Hone’s hypothesis that disease transmission occurs through the ingestion of *M. bovis* contaminated material). However, the ferret data were quite sparse, and a number of alternative models with p as a function of disease status had reasonable support. There was comparably little support for models with increased mortality for infected animals; however, simulation results indicated relatively little ability to estimate this quantity with just five age classes.

We reiterate that snapshots of age-prevalence data are only appropriate for studies of endemic disease where the effects of environmental stochasticity on vital rates are

minimal. Inference from such data requires similar assumptions as for vertical life tables (Seber 1982), including a stable age structure (Caswell 2001) and constant recruitment. Numerous authors have urged caution in using life table data for inference about survival in naturally fluctuating populations (e.g., Anderson et al. 1981; Menkens and Boyce 1993; Conn et al. 2005). However, our simulations suggested that FOI estimators have reasonable properties when there is some variability in vital rates (we note that simulations still assumed that these processes were stationary). In this paper, we have addressed one assumption not usually addressed by life table approaches—namely, detectability. We believe this is useful, in the spirit of illustrating “... how successive approximations to reality can improve mathematical models which remain inevitably approximate” (Cohen 1973). Tests of other life table assumptions (e.g., negligible temporal stochasticity) require sampling populations at more than one point in time. We urge ecologists to consider both logistical constraints and possible assumption violations when selecting a sampling program and analysis approach.

Future research should be directed at developing methods that allow for different functional forms of FOI, including those that are dependent on contact rates between susceptible and infected individuals. Several longitudinal studies have found increased infection transition probabilities in areas with higher disease prevalence (e.g., Lachish et al. 2007; Ozgul et al. 2009), which is expected under horizontal transmission [see, for example, Caley et al. (2009) for a review of functional forms proposed for FOI in these cases]. However, direct estimation of transmission rates when FOI depends on the number of infected individuals is not trivial. Adaption of state space methods using complete data parameterizations (e.g., Schofield et al. 2009) may be useful in this regard. However, complex sampling algorithms may be needed to sample the posterior surface (Gibson and Renshaw 1998; O’Neill and Roberts 1999).

We suspect that problems with detectability hamper a number of other types of disease prevalence analyses. By paying closer attention to statistical sampling protocols that incorporate detectability, we hope that ecologists can increase the defensibility of their work while simultaneously deriving more robust parameter estimates. In this manner, we envision a better prediction of wildlife disease dynamics and an increased ability to prescribe effective disease management strategies for animal and plant populations.

Acknowledgments Funding for the first author was partially provided by NIH/NSF grant EF0622705. We are grateful to L. Bailey, D. Heisey, B. Kendall, A. Schueller, and an anonymous reviewer for helpful comments and suggestions on a previous draft.

References

- Anderson DR, Wywiałowski AP, Burnham KP (1981) Tests of the assumptions underlying life table methods for estimating parameters from cohort data. *Ecology* 62:1121–1124
- Arnason AN (1972) Parameter estimation for mark-recapture experiments on two populations subject to migration and death. *Res Popul Ecol* 13:97–113
- Arnason AN (1973) The estimation of population size, migration rates, and survival in a stratified population. *Res Popul Ecol* 15:1–8
- Brownie C, Hines JE, Nichols JD, Pollock KH, Hestbeck JB (1993) Capture-recapture studies for multiple strata including non-Markovian transitions. *Biometrics* 49:1173–1187
- Burnham KP, Anderson DR (2002) Model selection and multimodel inference: a practical information-theoretic approach, 2nd edn. Springer, New York
- Caley P, Hone J (2002) Estimating the force of infection; *Mycobacterium bovis* infection in feral ferrets *Mustela furo* in New Zealand. *J Anim Ecol* 71:44–54
- Caley P, Marion G, Hutchings MR (2009) Assessment of transmission rates and routes, and the implications for management. In: Delahey RJ, Smith GC, Hutchings MR (eds) Management of disease in wild mammals. Springer, New York, pp 31–51
- Caswell H (2001) Matrix population models, 2nd edn. Sinauer, Sunderland
- Cohen JE (1973) Selective host mortality in a catalytic model applied to schistosomiasis. *Am Nat* 107:199–212
- Conn PB, Diefenbach DR (2007) Adjusting age and stage distributions for misclassification errors. *Ecology* 88:1977–1983
- Conn PB, Doherty Jr PF, Nichols JD (2005) Comparative demography of new world populations of thrushes (*turdus* spp.): comment. *Ecology* 86:2536–2541
- Conn PB, Arthur AD, Bailey LL, Singleton GR (2006) Estimating the abundance of mouse populations of known size: promises and pitfalls of new methods. *Ecol Appl* 16:829–837
- Cox DR, Oakes D (1984) Analysis of survival data. Chapman & Hall/CRC, Boca Raton
- Dhondt AA, Altizer S, Cooch EG, Davis AK, Dobson A, Driscoll MJL, Hartup BK, Hawley DM, Hochachka WM, Hosseini PR, Jennelle CS, Kollias GV, Ley DH, Swarthout ECH, Sydeman KV (2005) Dynamics of a novel pathogen in an avian host: mycoplasmal conjunctivitis in house finches. *Acta Trop* 94:77–95
- Ergon T, Yoccoz NG, Nichols JD (2009) Estimating latent time of maturation and survival costs of reproduction in continuous time from capture-recapture data. In: Thomson DL, Cooch EG, Conroy MJ (eds) Modeling demographic processes in marked populations, environmental and ecological statistics series, vol 3. Springer, New York, pp 173–197
- Faustino CR, Jennelle CS, Connolly V, Davis AK, Swarthout EC, Dhondt AA, Cooch EG (2004) Infection dynamics in a house finch population: seasonal variation in survival, encounter, and transmission rate. *J Anim Ecol* 73:651–669
- Gauthier DT, Latour RJ, Heisey DM, Bonzek CF, Gartland J, Burge EJ, Vogelbein WK (2008) Mycobacteriosis-associated mortality in wild striped bass (*Marone saxatilis*) from Chesapeake Bay, USA. *Ecol Appl* 18:1718–1727
- Gibson GJ, Renshaw E (1998) Estimating parameters in stochastic compartmental models using markov chain methods. *IMA J Math Appl Med Biol* 15:19–40
- Heisey DM, Joly DO, Messier F (2006) The fitting of general force-of-infection models to wildlife disease prevalence data. *Ecology* 87:2356–2365
- Hestbeck JB, Nichols JD, Malecki RA (1991) Estimates of movement and site fidelity using mark-resight data of wintering Canada geese. *Ecology* 72:523–533
- Hudson PJ, Dobson AP (1997) Transmission dynamics and host-parasite interaction of *Trichostrongylus tenuis* in red grouse *Lagopus lagopus scoticus*. *J Parasitol* 83:194–202
- Jennelle CS, Cooch EG, Conroy MJ, Senar JC (2007) State-specific detection probabilities and disease prevalence. *Ecol Appl* 17:154–167
- Joe M, Pollock KH (2002) Separation of survival and movement rates in multi-state tag–return and capture–recapture models. *J Appl Stat* 29:373–384
- Kalbfleisch JD, Lawless JF (1985) The analysis of panel data under a markov assumption. *J Am Stat Assoc* 80:863–871
- Keiding N (1991) Age-specific incidence and prevalence: a statistical perspective. *J R Stat Soc A* 154:371–412
- Kery M, Gregg KB (2003) Effects of life-state on detectability in a demographic study of the terrestrial orchid *Cleistes bifaria*. *J Ecol* 91:265–273
- Lachish S, Jones M, McCallum H (2007) The impact of disease on the survival and population growth rate of the Tasmanian devil. *J Anim Ecol* 76:926–936
- Menkens JGE, Boyce MS (1993) Comments on the use of time-specific and cohort life tables. *Ecology* 74:2164–2168
- Miller TJ, Andersen PK (2008) A finite-state continuous-time approach for inferring regional migration and mortality rates from archival tagging and conventional tag-recovery experiments. *Biometrics* 64:1196–1206
- Muench H (1959) Catalytic models in epidemiology. Harvard University Press, Cambridge
- O'Neill PD, Roberts GO (1999) Bayesian inference for partially observed stochastic epidemics. *J R Stat Soc A* 162:121–129
- Otis DL, Burnham KP, White GC, Anderson DR (1978) Statistical inference from capture data on closed populations. *Wildl Monogr* 62:3–135
- Ozgul A, Oli MK, Bolker BM, Perez-Heydrich C (2009) Upper respiratory tract disease, force of infection, and effects on survival of gopher tortoises. *Ecol Appl* 19:786–798
- Pledger S (2000) Unified maximum likelihood estimates for closed capture-recapture models using mixtures. *Biometrics* 56:434–442
- R Development Core Team (2005) R: a language and environment for statistical computing. R Foundation for Statistical Computing, Vienna, Austria, <http://www.R-project.org>. Accessed November 2009
- Renshaw E (1991) Modelling biological populations in space and time. Cambridge University Press, Cambridge
- Schofield MR, Barker RJ, MacKenzie DI (2009) Flexible hierarchical mark-recapture for open populations using Winbugs. *Environ Ecol Stat* 16:369–387
- Schwarz CJ, Schweigert JF, Arnason AN (1993) Estimating migration rates using tag–recovery data. *Biometrics* 49:177–193
- Seber GAF (1982) The estimation of animal abundance and related parameters, 2nd edn. Blackburn Press, Caldwell
- Taylor HM, Karlin S (1984) An introduction to stochastic modeling. Academic Press, New York
- Woolhouse MEJ, Chandiwana SK (1992) A further model for temporal patterns in the epidemiology of schistosome infections of snails. *Parasitology* 104:443–449
- Zippin C (1956) An evaluation of the removal method of estimating animal populations. *Biometrics* 12:163–189